Jamming in Sheared Foams and Emulsions, Explained by Critical Instability of the Films between Neighboring Bubbles and Drops

N. D. Denkov,[1,*] S. Tcholakova,[1] K. Golemanov,[1] and A. Lips[2]

[1]*Laboratory of Chemical Physics and Engineering, Faculty of Chemistry, Sofia University, Bulgaria*

[2]*Unilever Discover, Port Sunlight Laboratory, CH63 3JW, Wirral, United Kingdom*

(Received 16 January 2009; published 10 September 2009)

Foam and emulsion jamming at low shear rates is explained by considering the thinning dynamics of the transient films, formed between neighboring bubbles and drops. After thinning gradually to a critical thickness, these films undergo an instability transition, which leads to the formation of very thin "black films" providing strong adhesion between the dispersed particles. Analysis shows that such film thickness instability occurs only if the contact time between particles is sufficiently long—an explicit expression for the respective critical shear rate is derived and compared to experimental data.

DOI: 10.1103/PhysRevLett.103.118302 PACS numbers: 83.80.Iz, 47.57.Bc, 82.70.Rr, 83.60.Wc

Nonhomogeneous flow, often discussed in terms of "shear-banding" or "jamming-unjamming transitions," has attracted researchers' attention because it appears as a generic phenomenon in various systems, such as glassy and granular materials, concentrated suspensions, foams, emulsions, and micellar solutions [1–10]. This phenomenon is still poorly understood, and appropriate theoretical modeling, beyond phenomenological description, is missing. Foams and emulsions seem particularly suitable for studying nonhomogenous flows and related phenomena, because the behavior of these systems is governed by a relatively well understood interplay of capillary effects and viscous friction in the films, formed between neighboring bubbles and drops [11–15]. This understanding provides the unique possibility for detailed theoretical modeling and experimental studies of these systems at the microstructural level (viz., at the level of single drops, bubbles, and films), which is impossible for the other systems of interest.

Recently, several systematic studies were performed [1–10] to clarify the main factors controlling jamming or unjamming transitions in foams and emulsions. Some of the conclusions relevant to the current study are that (i) jamming is observed at a certain "critical" shear rate—when this critical rate is reached from above, the bubbles or drops in the dispersion "stick" to each other, thus creating jammed zones—and (ii) the critical shear rate depends on several factors, such as the drop and bubble size, the volume fraction, and, most importantly, the interaction between dispersed particles. The effect of interparticle forces was demonstrated with moderately concentrated emulsions, for which jamming transition was observed only in systems with attractive interdroplet forces [10]. Until now these observations lack clear explanations and quantitative description.

The main goal of this Letter is to demonstrate that jamming (liquid-to-solid) transitions in flowing foams and emulsions could be explained by considering the dynamics of thinning of the films, formed between neighboring bubbles and drops. For brevity, we discuss explicitly mostly bubbles in foams; however, the analysis is applicable to concentrated emulsions containing micrometer drops, provided that the appropriate system parameters are used.

The dynamics of film thinning was analyzed in Refs. [11,12] in relation to viscous dissipation in steadily sheared foams and emulsions. As in [11,12], we consider the processes of film formation and thinning between bubbles, located in two neighboring planes of sheared foam. These planes are assumed to slide along each other with constant relative velocity, u (see Fig. 1). The foam shear rate can be expressed as $\dot{\gamma} = 0.676u\Phi^{1/3}/R_0$, and the capillary number is $\mathrm{Ca} \equiv (\mu\dot{\gamma}R_0/\sigma)$.

In such sheared foams, planar foam films with initial thickness, h_0, are formed when the hydrodynamic pressure in the gap between colliding bubbles becomes equal to bubble capillary pressure, $P_d(h_0) = P_C$, where $P_C(\Phi)$ is the known function of the bubble volume fraction, Φ [13–16]. From this pressure balance one can derive an expression for the initial film thickness, $h_0 \approx (3\mu u/8\sigma)^{1/2}R_N$, where μ is dynamic viscosity of continuous phase, σ is interfacial tension, and $R_N = 2\sigma/P_C$ is radius of curvature of the bubble surface in the contact zone, just before film formation [12,15].

The radius of the transient foam film, formed between two bubbles during their contact, $R_F(t)$, gradually in-

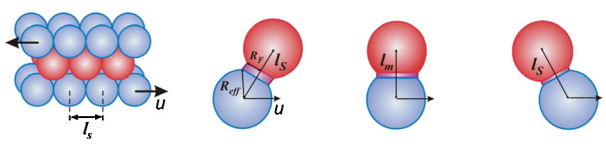

FIG. 1 (color online). Schematic presentation of the relative motion of neighboring planes of bubbles in sheared foam, and of the related process of film formation and thinning between two neighboring bubbles.

creases from its initial value, $R_{F0} = (h_0 R_N)^{1/2}$, to a maximal value when the bubbles are closest to each other, and then decreases down to zero as the bubbles separate, dragged by the flow [11,12]. For the calculations involving $R_F(t)$, it is convenient to introduce an effective bubble size, $R_{\text{eff}} = (R_{FS}^2 + l_S^2/4)^{1/2}$, which is defined as the radius of a spherical surface with just one film (instead of the 12 films in the assumed fcc structure) that has the same ratio R_{FS}/l_S, as the deformed polyhedral bubbles in the actual foam [12]. Here $R_{FS}(\Phi)$ is film radius [12,13] and $l_S \approx 1.812 R_0/\Phi^{1/3}$ is center-to-center distance in the static nonsheared foam. Thus we replace the real polyhedral bubbles in sheared foam by "imaginary" bubbles having just one foam film in the zone of contact, which leads [12] to the following expression for the film radius, $R_F(t) = [R_{\text{eff}}^2 - l(t)^2/4]^{1/2}$. Here $l(t) = [l_m^2 + (ut - \sqrt{l_0^2 - l_m^2})^2]^{1/2}$ is distance between bubble geometrical centers, $l_m = l_S\sqrt{3}/2$ is the respective minimum distance, and $l_0 = l(t = 0)$ is the distance in the moment of film formation.

The theoretical analysis shows [12] that the film thickness, $h(t)$, obeys Reynolds equation

$$(dh/dt) = -2[P_C - \Pi(h)]h^3/3\mu R_F^2, \tag{1}$$

where $\Pi(h)$ is disjoining pressure, which accounts for the forces acting between foam film surfaces (such as van der Waals, electrostatic, depletion, etc. [17,18]). For simplicity, below we consider explicitly only van der Waals attraction, characterized by the Hamaker constant, A_H [17,18]:

$$\Pi(h) = -A_H/6\pi h^3 \tag{2}$$

It is well known from literature [14,19–23] that in the presence of attractive forces the thinning of foam and emulsion films down to a certain critical thickness, h_{CR}, leads to a spontaneous jump to a very small thickness, often corresponding to two surfactant monolayers, stabilizing the film by short-range steric repulsion (see Fig. 2). This jump is driven by attractive interactions and has been studied extensively in relation to coalescence stability of foams and emulsions [19–22]. The formed ultrathin films, with thickness between ca. 4 and 10 nm, are called "black films" (BFs), because they appear dark when observed in reflected light. BFs are characterized by strong attraction between film surfaces and are thus able to withstand a certain detachment force [14,20,22]. Therefore, the BF formation leads to adhesion between neighboring bubbles (drops), which could jam locally the foam (emulsion).

The spontaneous jump in film thickness at h_{CR} is driven by attractive surface forces, and the following explicit formula for h_{CR} was derived for dominant van der Waals interactions [19]:

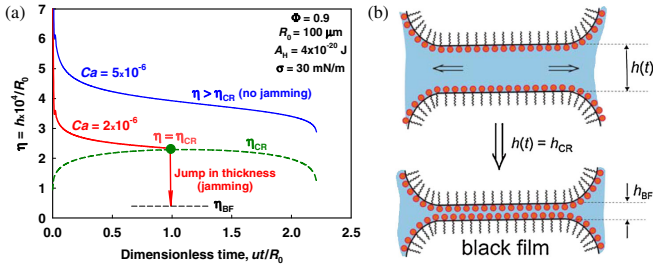

FIG. 2 (color online). (a) Calculated dimensionless thickness, $\eta = h/R_0$, of the foam film between two neighboring bubbles in sheared foam, as a function of dimensionless time after film formation, ut/R_0, for two shear rates (solid curves), compared to dimensionless critical film thickness, $\eta_{\text{CR}} = h_{\text{CR}}/R_0$ (dashed curve). The transient film thickness, $h(t)$, becomes equal to h_{CR} only below a certain capillary number (shear rate). (b) Schematic presentation of the thinning of the foam film between two bubbles. After the spontaneous jump in film thickness at $h(t) = h_{\text{CR}}$, the formed very thin (black) film is stabilized by short-range repulsive forces, while the long-range attractive forces lead to adhesion between film surfaces [17,18,20,22].

$$h_{\text{CR}} = 0.21\left(\frac{A_H^2 R_F^2}{\sigma P_C}\right)^{1/7}. \tag{3}$$

Equations (1)–(3) provide the theoretical basis for considering the effect of film thinning on foam and emulsion jamming in the case of prevailing van der Waals interactions [the same approach can be used for other interactions, at known $\Pi(h)$]. Comparing the thickness of the dynamic film, formed between two neighboring bubbles in sheared foam, $h(t)$, with the critical film thickness, h_{CR}, one can determine whether the foam film will spontaneously jump to form BF while the bubbles pass by each other, thus inducing strong bubble-bubble adhesion. Such a comparison is illustrated in Fig. 2, with parameter values typical for bubbles in sheared foams.

As seen from Fig. 2(a), $h(t) = h_{\text{CR}}$ when $R_F(t)$ is close to its maximum, viz., at dimensionless time $\tilde{t} = ut/R_0 \approx 1$. This observation allows us to derive approximate expressions for the critical shear rate, $\dot{\gamma}_{\text{jam}}$, and critical capillary number, Ca_{jam}, leading to a spontaneous jump in the film thickness and, thereby, to foam jamming. With this aim in view, we first integrate Eq. (1) at negligible disjoining pressure, $\Pi(h) \ll P_C$, to obtain the following expression for the film thickness [11,12]:

$$\frac{1}{h^2} = \frac{1}{h_0^2} + \frac{16P_C}{3\mu}\frac{1}{u\sqrt{4R_{\text{eff}}^2 - l_m^2}}\left[\text{arctanh}\left(\frac{\sqrt{l_0^2 - l_m^2}}{\sqrt{4R_{\text{eff}}^2 - l_m^2}}\right) + \text{arctanh}\left(\frac{ut - \sqrt{l_0^2 - l_m^2}}{\sqrt{4R_{\text{eff}}^2 - l_m^2}}\right)\right]. \tag{4}$$

Note that the attractive van der Waals forces are neglected in Eq. (4), which is, therefore, only an approximation to the

more precise result, which is obtained by numerical integration of Eq. (1). Next, we estimate from Eq. (4) the film thickness in moment $\tilde{t} = 1$ (viz., at $l = l_m$), taking into account the fact that the term with h_0 is usually negligible (because $h_0 \gg h_{CR}$) and the second term in the square brackets is identically zero in this moment, thus obtaining $h(\tilde{t} = 1) \approx 0.18(R_N R_0 \mathrm{Ca})^{1/2}$.

Next we use the relation between R_N and bubble capillary pressure, $R_N = 2\sigma/P_C$, to derive an approximate interpolating formula, $R_N \approx 1.86R_0(1 - \Phi)^{0.4}$, from a known expression for P_C [16] (this formula for R_N is valid for $0.80 \leq \Phi \leq 0.98$). Finally, we note that the film radius at $\tilde{t} = 1$ could be approximated as $R_F(\tilde{t} = 1) \approx R_0/2$ for not-very-low-volume fractions. Combining all these expressions with the condition for film instability, $h(\tilde{t} \approx 1) = h_{CR}$, we derive the following explicit expressions for the critical shear rate and the critical capillary number leading to foam and emulsion jamming:

$$\mathrm{Ca}_{\mathrm{jam}} = \frac{0.43}{(1 - \Phi)^{0.3}} \left(\frac{A_H}{\sigma R_0^2} \right)^{4/7}, \tag{5}$$

$$\dot{\gamma}_{\mathrm{jam}} = 0.43 \frac{\sigma^{3/7} A_H^{4/7}}{\mu R_0^{15/7} (1 - \Phi)^{0.3}} \tag{6}$$

Equations (5) and (6) were compared with the numerical results from the integration of Eq. (1), taking into account the correct dependence of R_F on Φ, and were found to give correct values within 10%–15% for bubble volume fractions $0.80 \leq \Phi \leq 0.98$ and capillary numbers, $10^{-8} < \mathrm{Ca}_{\mathrm{jam}} < 10^{-4}$, which are of primary interest. Therefore, Eqs. (5) and (6) are appropriate and convenient for illustrating the main trends and for simple estimates.

Results from the numerical calculations for $\dot{\gamma}_{\mathrm{jam}}$ and $\mathrm{Ca}_{\mathrm{jam}}$, with parameters typical for foams, are shown in Fig. 3(a). One sees that the dependence of $\dot{\gamma}_{\mathrm{jam}}$ and $\mathrm{Ca}_{\mathrm{jam}}$ on the bubble volume fraction is relatively weak, whereas the dependence on the bubble size is significant. Similar calculations showed that the dependence of $\dot{\gamma}_{\mathrm{jam}}$ and $\mathrm{Ca}_{\mathrm{jam}}$ on the Hamaker constant, A_H, is also relatively weak, when

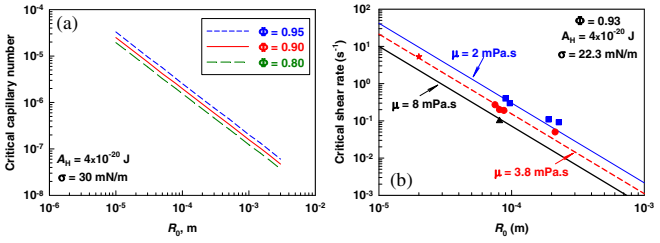

FIG. 3 (color online). (a) Numerical results for the dependence of $\mathrm{Ca}_{\mathrm{jam}}$ on bubble radius, R_0, at different bubble volume fractions, Φ, with Hamaker constant, A_H, and interfacial tension, σ, typical for foams. (b) Comparison of the theoretical prediction for $\dot{\gamma}_{\mathrm{jam}}$ (lines) with our experimental data obtained with foams (symbols). The star shows data obtained with shaving foam in [4].

A_H is varied in the typical range for foams and emulsions (between 4×10^{-21} and 4×10^{-20} J [17]). All these results are in a very good agreement with the approximate expressions, Eqs. (5) and (6), which also predict strong dependence on particle size and solution viscosity only.

To check these predictions, we performed experiments with foams sheared between the parallel plates of a rheometer Gemini (Malvern Instruments, UK). Sandpaper was glued on the plates to suppress foam-wall slip, and the periphery of the sheared foam was video-recorded, using a long-focus magnifying lens. The gap between the plates was 3 mm, whereas the average bubble radius was $\approx$ 100 to 200 μm. For each experiment, the velocity of more than 100 bubbles (with different vertical locations across the gap) was measured to reconstruct the foam velocity profile.

The observations showed that, at high shear rate, the foam flow is homogeneous, with the relative rate of the neighboring bubbles representing well the average shear rate. In contrast, at very low shear rate, the layers of bubbles close to the plates were jammed, and the foam flow was realized through the formation of a "slip" plane in the middle of the gap—the bubbles around this plane were jumping to the next positions, thus allowing for a relative motion of the two jammed zones attached to the plates.

Most interesting was the intermediate range of shear rates, in which a central zone was formed, where the bubbles were flowing with a constant shear rate, coexisting with two jammed zones attached to the plates. In line with [6] we found that the variation of the global shear rate in this regime leads to variation of the widths of these zones, whereas the shear rate in the middle zone remains approximately the same (lever rule) and corresponds to the lowest possible shear rate before the bubbles get jammed, $\dot{\gamma}_{\mathrm{jam}}$ (viz., to critical rate for liquid-to-solid transition). Thus we determined $\dot{\gamma}_{\mathrm{jam}}$ for a set of foams with different μ, mean bubble size, and foam polydispersity [24]. The obtained results are compared with model predictions in Fig. 3(b). One sees a very good agreement, without adjustable parameters used in the calculations (the slight deviation, observed for the biggest bubbles, is probably due to gravity effects). Reasonably good agreement was found also with the results obtained in [4] with shaving foams containing much smaller bubbles.

Note that Eqs. (5) and (6) are derived assuming negligible effects of gravity and surface forces on the film thinning process. These assumptions limit the range of equation validity to particle radii between ca. 2 and 200 μm, which is typical for many emulsions and foams. It is worthwhile noting, however, that the bubbles and drops studied in [8,10] are outside this size range, which explains why Eqs. (5) and (6) do not describe quantitatively these data, despite the observed qualitative agreement (as predicted, critical shear rate increased significantly with the decrease of particle size, and jam-

ming was observed in presence of attractive forces only [8,10]).

Two features of our model deserve special attention: First, the model predicts that the conditions for jamming depend weakly on Φ and on the specific particle arrangement at the microstructural level. These predictions seem adequate when describing dispersions of soft particles, because the particle deformability allows uniform distribution of the stress toward all neighbors and precludes sharp dependence (divergence) of the dispersion mechanical characteristics around the particle close-packing, Φ_{CP}. In contrast, for solid particles, the dependence on Φ is known to be strong around Φ_{CP} [9,18], and local topological effects could be very significant. Second, the model explains the jamming transition with formation of thin black films in the jammed zone, viz., as related to significant structural change in the system at the transition.

In conclusion, we explain jamming (liquid-to-solid) transition in sheared foams and concentrated emulsions by critical instability of the films, formed between the neighboring bubbles and drops. This instability leads to a spontaneous jump in film thickness, at a certain critical thickness, h_{CR}, with a subsequent formation of very thin BFs which are characterized with strong adhesion between the film surfaces. For this film instability to occur, the film should have enough time to thin down to h_{CR} during the period of particle contact. The latter requirement allows us to calculate the critical shear rate, $\dot{\gamma}_{jam}$ (and the corresponding capillary number Ca_{jam}), leading to formation of BF and dispersion jamming, if the attractive surface forces between the particles are known. For dominant van der Waals forces, the model predicts that Ca_{jam} depends mostly on particle size and on the magnitude of attractive forces [Eq. (5)]. The model predictions agree well with experimental data without using adjustable parameters. This agreement proves that properly chosen foams, with bubble radius in the range of ca. 20–150 μm, are indeed very appropriate for quantitative investigation of jamming and the related phenomena, because the bubble dynamics could be described theoretically in great detail and could be observed directly with optical devices.

After modifications, the same approach could be applied to other types of dispersions, such as suspensions of soft particles (vesicles, microgel particles) or spherical solid particles [1,2,4,6]. For this purpose, appropriate material parameters and expressions for the surface forces should be implemented in the consideration. Note that the description of the related unjamming (solid-to-liquid) transition requires a different approach, because the process of particle detachment against the adhesion forces should be considered—this more difficult task is postponed for a subsequent study.

This study is supported by Project No. Rila-422/2008 with the National Science Fund of Bulgaria, and is related to the activities of COST P21 action ''Physics of Drops'' and of Unilever Discover Trumbull, CT, USA.

*Corresponding author.
nd@lcpe.uni-sofia.bg

[1] P. Coussot *et al.*, Phys. Rev. Lett. **88**, 218301 (2002).
[2] F. Da Cruz, F. Chevoir, D. Bonn, and P. Coussot, Phys. Rev. E **66**, 051305 (2002).
[3] V. J. Langlois, S. Hutzler, and D. Weaire, Phys. Rev. E **78**, 021401 (2008).
[4] S. Rodts, J. C. Baudez, and P. Coussot, Europhys. Lett. **69** 636 (2005); J. C. Baudez and P. Coussot, Phys. Rev. Lett. **93**, 128302 (2004).
[5] G. Katgert, M. E. Möbius, and M. van Hecke, Phys. Rev. Lett. **101**, 058301 (2008).
[6] P. C. F. Moller, S. Rodts, M. A. J. Michels, and D. Bonn, Phys. Rev. E **77**, 041507 (2008).
[7] J. Lauridsen, G. Chanan, and M. Dennin, Phys. Rev. Lett. **93**, 018303 (2004).
[8] C. Gilbreth, S. Sullivan, and M. Dennin, Phys. Rev. E **74**, 051406 (2006).
[9] M. Dennin, J. Phys. Condens. Matter **20**, 283 103 (2008).
[10] L. Becu, S. Manneville, and A. Colin, Phys. Rev. Lett. **96**, 138302 (2006).
[11] N. D. Denkov *et al.*, Phys. Rev. Lett. **100**, 138301 (2008).
[12] S. Tcholakova *et al.*, Phys. Rev. E **78**, 011405 (2008).
[13] H. M. Princen, in *Encyclopedia of Emulsion Technology*, edited by J. Sjöblom (Marcel Dekker, New York, 2001), Chap. 11, p. 243.
[14] I. B. Ivanov, Pure Appl. Chem. **52**, 1241 (1980).
[15] D. S. Valkovska, K. D. Danov, and I. B. Ivanov, Colloids Surf. A **156**, 547 (1999).
[16] R. Hohler, Y. Y. C. Sang, E. Lorenceau, and S. Cohen-Addad, Langmuir **24**, 418 (2008).
[17] J. N. Israelachvili, *Intermolecular and Surface Forces* (Academic Press, New York, 1992), 2nd ed.
[18] P. A. Kralchevsky, K. D. Danov, and N. D. Denkov, *In Handbook of Surface and Colloid Chemistry*, edited by K. S. Birdi (CRC Press LLS, Boca Raton, 1997), Chap. 11.
[19] A. Vrij, Discuss. Faraday Soc. **42**, 23 (1966).
[20] A. Scheludko, Adv. Colloid Interface Sci. **1**, 391 (1967).
[21] I. B. Ivanov, B. Radoev, E. Manev, and A. Scheludko, Trans. Faraday Soc. **66**, 1262 (1970).
[22] D. Exerowa and P. M. Kruglyakov, *Foams and Foam Films: Theory, Experiment, Application* (Elsevier, Amsterdam, 1998).
[23] D. S. Valkovska, K. D. Danov, and I. B. Ivanov, Adv. Colloid Interface Sci. **96**, 101 (2002).
[24] Experiments with foams of different polydispersity (relative width of bubble-size distribution varied between 0.15 and 0.95) showed that harmonic-mean bubble radius, $R_h = [(\sum 1/R)/N]^{-1}$, which emphasizes the contribution of the small bubbles, should be used as the mean bubble radius for such foams. The reason is that the films formed with participation of small bubbles thin more rapidly; hence, small bubbles promote jamming by acting as ''glue'' particles for the bigger bubbles.